The Lifespan Trajectories of Brain Activities Related to Cognitive Control

Zhenghan Li[1,2,3,4], Isaac T. Petersen[5], Lingxiao Wang[6,7,3], Joaquim Radua[8,9,10], Guochun Yang[5,11,4*], Xun Liu[4,12]

[1] Institute of Brain Science and Department of Physiology, School of Basic Medical Sciences, Hangzhou Normal University, Hangzhou, China

[2] Zhejiang Philosophy and Social Science Laboratory for Research in Early Development and Childcare, Hangzhou Normal University, Hangzhou, China

[3] Zhejiang Key Laboratory for Research in Assessment of Cognitive Impairments, Hangzhou, China

[4] Key Laboratory of Behavioral Science, Institute of Psychology, Chinese Academy of Sciences, Beijing, China

[5] Department of Psychological and Brain Sciences, University of Iowa, Iowa City, IA, USA

[6] Centre for Cognition and Brain disorders, The Affiliated Hospital of Hangzhou Normal University, Hangzhou, Zhejiang Province, China

[7] Institute of Psychological Science, Hangzhou Normal University, Hangzhou, Zhejiang Province, China

[8] Institut d'Investigacions Biomèdiques August Pi i Sunyer (IDIBAPS), CIBERSAM, University of Barcelona, Barcelona, Spain

[9] Institute of Psychiatry, Psychology and Neuroscience, King's College London, London, United Kingdom

[10] Department of Clinical Neuroscience, Karolinska Institute, Stockholm, Sweden

[11] Cognitive Control Collaborative, University of Iowa, Iowa City, IA, USA

[12] Department of Psychology, University of Chinese Academy of Sciences, Beijing, China

*__Correspondence:__ guochun-yang@uiowa.edu

Classification: Biological Sciences/Psychological and Cognitive Sciences

Keywords: Cognitive control; Lifespan; Brain activity; Neuroimaging meta-analysis; Heterogeneity

Abstract

Cognitive control plays a pivotal role in guiding human goal-directed behavior. While existing studies have documented an inverted U-shaped trajectory of cognitive control both behaviorally and anatomically, little is known about the corresponding changes in functional brain activation with age. To bridge this gap, we conducted a comprehensive meta-analysis of 129 neuroimaging studies using conflict tasks, encompassing 3,388 participants aged from 5 to 85 years old. We have three major findings: 1) The inverted U-shaped trajectory is the predominant pattern; 2) Cognitive control-related brain regions exhibit heterogeneous lifespan trajectories: the frontoparietal control network follows inverted U-shaped trajectories, peaking between 24 and 40 years, while the dorsal attention network demonstrates no clear trajectories; 3) Both the youth and the elderly show weaker brain activities and greater left laterality than young to middle-aged adults. These results reveal the lifespan trajectories of cognitive control, highlighting heterogeneous fluctuations in brain networks with age.

Introduction

The cognitive abilities of human beings dynamically change throughout the entire lifespan, experiencing rapid development in the early stages, and gradual decline in the later period of life. As one of the most fundamental cognitive functions, cognitive control is deeply engaged in various domains of high-level capabilities that humans greatly outperform other species, such as decision making, planning and problem solving[1]. Cognitive control refers to the cognitive processes that enable individuals to manage and regulate their attention, thoughts, and actions, which plays a vital role in goal-directed behavior, allowing us to focus on the target and ignore distractors[2,3]. For instance, cognitive control enables us to concentrate on reading in a library despite the presence of people chatting nearby.

Cognitive control provides fundamental support for normal human behaviors. Young adults typically maintain an optimal mature level of cognitive control[4]. However, the youth (including children and adolescents, less than 18 years) and elderly (60 years and older) individuals may struggle with behavioral problems because of their suboptimal cognitive control system[5-10]. While the state-of-art progress of cognitive/behavioral changes has been well-documented and shaped how the diagnosis of developmental/ageing related disorders[11], the change of related neural system has been under-investigated. Understanding how the neural underpinning of cognitive control changes

over the lifespan can yield valuable insights into the developmental and aging mechanisms of the human brain. This knowledge may assist in customizing cognitive training strategies based on related brain regions and their activities[12].

Researchers generally believe that cognitive control ability follows an inverted U-shaped trajectory across the lifespan[5,13,14,17]. This inverted U-shaped trajectory has been generally supported by behavioral and anatomical evidence. The Eriksen Flanker task (requiring participants to respond to central stimuli while ignoring flanking distractions) has been widely utilized to detect cognitive control across the lifespan[15], and results suggest a clear U-shape trajectory of conflict cost (measured by worsened behavioral performance, e.g., reaction time, in incongruent compared to congruent conditions) with age[16-18]. Similar results have been observed in other conflict tasks, such as color-word Stroop (requiring participants to name the ink color of a word that is incongruent with the word's semantic meaning)[16]. Recent large-cohort studies have also found that gray and white matter volumes across all brain regions exhibit overall inverted U-shaped trajectories with age, with the gray matter volume peaking at early adolescence and the white matter volume peaking at young adulthood[19,20]. During late adulthood, normal ageing yields a protracted decline of brain structure, with the volumes of both gray matter and white matter reduced[14]. Consistently, the gray matter volumes of the frontal and parietal regions, which are essential in cognitive control tasks[21], have also been found to increase during early childhood and atrophy in early elderly age[22].

However, it remains largely unknown how brain activities related to cognitive control change over the lifespan. Previous research has primarily focused on brain activities in either youths or elderly adults, rather than examining changes across the entire lifespan. With conflict paradigms, children and adolescents are often found to have lower brain activity than young adults in frontoparietal regions (refs.[23-28], but see Bunge et al. [29]). For example, a study utilizing the Flanker task revealed that children aged 8−12 years had reduced activation in dorsolateral prefrontal regions compared to young adults, suggesting an immature cognitive control system[27]. However, brain activity differences in elderly adults as compared to young adults during cognitive control tasks have been less consistently reported[14]. Some studies have found that elderly adults have lower neural activity in frontoparietal regions than young adults[30-32], possibly because elderly adults may be unable to engage in an equal level of control-related activity due to functional decline. On the other hand, other studies have found that elderly adults may exhibit greater brain activity in frontoparietal regions than young adults[33,34], possibly because they have recruited additional brain regions to compensate for their decreased efficiency in utilizing control resources. Adding to the debate, it has been proposed that the cognitive control function in elderly adults might not decline at all[35,36]. These conflicting findings underscore the complexity of understanding age-related differences in cognitive control.

Few studies have directly tested the change of brain activities related to cognitive control across the lifespan. One existing study observed a positive association between

the activation of the bilateral prefrontal cortex and age[37]. Given the relatively small sample size (N = 30), the reliability of these findings is somewhat limited. As a result, it is difficult to draw a clear conclusion about how brain activities related to cognitive control change across the entire age range.

One direct way to test the lifespan trajectory of brain activation related to cognitive control is to conduct a large cohort of neuroimaging study with participants covering a wide age range. To the best of our knowledge, such studies have not yet been conducted. An alternative approach is to utilize meta-analyses to combine the results of existing studies targeting different age groups. Compared to the large cohort studies, meta-analyses are more accessible and resource-saving. In addition, meta-analyses can increase the statistical power and generalizability by combining various studies, reducing heterogeneity and bias from individual studies' methods, populations, or confounding variables[38]. Importantly, meta-analyses can reveal patterns not evident in individual studies, like nonlinear effects or interactions[38]. Several neuroimaging meta-analyses have examined age-related changes of cognitive control brain activity[31,39,40], but limitations such as incomplete age coverage and insufficient studies in certain age ranges prevent them from appropriately answering questions about the lifespan trajectory of cognitive control functions[31,39,40]. These studies have primarily focused on spatial convergence and/or diversity of coordinates across different age ranges, offering limited insights into lifespan trajectories of activity strength. Although a few studies have attempted para-

metric meta-regression to examine the age-related differences in cognitive control-related brain activity[39,41], they have been constrained by utilizing linear models that may overlook non-linear trajectory patterns, such as the inverted U-shaped trend.

The goal of this study is to provide a comprehensive examination to reveal the lifespan trajectory of brain activities responsible for cognitive control. Instead of encompassing various aspects of cognitive control, we focus on conflict processing for several reasons. First, conflict processing reflects the fundamental cognitive control ability to maintain a goal while avoiding distractions[2]. Second, its mechanisms in young adults are relatively well-known, with the frontoparietal and cingulo-opercular networks engaged[21,42], providing a baseline reference for our study. Third, conflict tasks with neuroimaging data have been widely applied to both younger and elderly groups, making a systematic meta-analysis feasible. Lastly, different conflict tasks share key components of cognitive control, such as conflict monitoring[43] and inhibitory control[8], which enables us to conduct effect-size-based meta-analyses using the congruency effect (i.e., the contrast between incongruent and congruent/neutral conditions). Including other sub-processes of cognitive control may introduce heterogeneity and make effect sizes incomparable.

Previous research suggests that better cognitive control-related performance is often associated with greater brain activity, especially in the prefrontal cortex[44]. Therefore,

we hypothesized that brain activities related to cognitive control might follow an inverted U-shaped trajectory like that of behavior patterns. Additionally, we hypothesized that different brain networks may show some heterogeneity in their lifespan trajectories.

Results

Sample Description

A total of 3,611 articles were identified including 3,484 articles searched from the database, 111 articles adopted from a previous study[21], and 16 articles searched from the references of crucial articles. After excluding duplicates and applying exclusion criteria, 119 articles including 129 studies with 3,388 participants and 1,579 brain activation foci, were included in this meta-analytic study (Supplementary Fig. S1 and Table S1). The average age of participants ranged from 8 to 74 years, with the individual age ranging from 5 to 85 years. A demonstration of the age distribution for each included study is presented in Supplementary Fig. S2.

Regions Related to Cognitive Control Identified by both ALE and SDM

To enhance the replicability and robustness of our finding and enable direct comparison with a previous study[21], we conducted the mean analysis across all studies with the activation likelihood estimation (ALE) and seed-based d mapping (SDM) approaches separately. First, we performed the single dataset analysis with the GingerALE software

166 to explore the brain regions consistently reported in all the included studies (see section
167 "*Activation Likelihood Estimation (ALE)*" in Methods). Results showed significant ac-
168 tivation in the frontoparietal regions, including the left dorsolateral prefrontal cortex,
169 bilateral frontal eye field, right inferior frontal gyrus and bilateral inferior parietal lob-
170 ule; the cingulo-opercular regions, including the supplementary motor area and bilateral
171 insula; and other regions, including the left inferior temporal gyri (Fig. 1A and Supple-
172 mentary Table S2). Second, we calculated the average brain activation based on the
173 effect sizes reported in all studies using the SDM with permutation of subject images
174 (SDM-PSI) software (see section "*Mean Analyses Across all Studies*" in Methods).
175 Similar to the ALE results, we found significant activation in the frontoparietal regions
176 (left inferior parietal lobule, right inferior frontal gyrus, and right middle frontal gyrus),
177 the cingulo-opercular regions (left anterior cingulate cortex), and other regions includ-
178 ing bilateral inferior temporal gyrus, right caudate nucleus, right cerebellum, and left
179 anterior thalamic projections (Fig. 1B and Supplementary Table S3). The count of
180 voxels revealed that the overlapped area (3,496 voxels, Fig. 1C) accounted for 96.3%
181 of the regions from the ALE analysis (3,635 voxels), and 15.0% of the regions from the
182 SDM analysis (23,240 voxels). This result suggested that SDM analysis could be a re-
183 liable approach for detecting brain regions, thereby laying a solid foundation for using
184 this approach in subsequent analyses. In addition, a robustness analysis suggested that
185 age does not influence the mean results of SDM analysis (Supplementary Fig. S3 and
186 Table S2).

[Fig. 1]

Trajectories of Cognitive Control Regions Identified in the Mean Analysis

Having identified nine brain regions in the mean analysis using SDM-PSI, we proceeded to explore how the activation levels of these regions change with age. To this end, we extracted brain activity data from all studies for each identified region. Before performing the meta-regression, we verified the effectiveness of using mean age as a predictor with a simulation approach (Supplementary Note S1 and Fig. S4). We then subjected the extracted data to separate generalized additive model (GAM) analyses, factoring in the confounding covariates (see section "*Generalized Additive Model (GAM) Fitting*" in Methods). The analyses (Supplementary Table S4) revealed significant age-related changes in the activation levels of 4 out of the 9 regions (Fig. 2, l-ACC, r-IFG, l-ITG, and r-CN). Visualization of the trajectories suggests that these regions showed inverted U-shaped patterns. The significance of their inverted U-shaped trajectories was further examined using a two-line test approach[45]. Results suggest that all four regions involve an increase in activity from childhood to young adulthood (approximately up to 30 years of age), and three of them (r-IFG, l-ITG and r-CN) showed consistent decrease in the later stages of age (Supplementary Note S2). The other five regions (Fig. 2, l-IPL, r-ITG, r-MFG, r-CB and l-ATP) showed no significant age-related changes. Notably, none of the clusters showed significant publication bias based on Egger's test (ps > 0.86), and they all showed low between-study heterogeneity (τs <

207 0.13, Qs < 12.11, I^2s < 25%). This indicates that the observed results are not likely
208 influenced by biased reporting or substantial variability in the included studies. A ro-
209 bustness analysis further ruled out the potential influence of including unpublished and
210 non-English studies in this study (Supplementary Note S4 and Fig. S5).

211 [Fig. 2]

212 Note that some regions are large, containing up to over 9,000 voxels. This could
213 obscure the distinct trajectories specific to different subregions, which are crucial in
214 understanding the hierarchical patterns of lifespan trajectories. We address this by using
215 a more granular approach below.

216 **Detecting Different Trajectories of Whole Brain Activities**

217 To explore various possibilities of lifespan trajectories, we grouped studies by their
218 mean age into the youth, young to middle-aged, and elderly groups, and then conducted
219 several contrast analyses (see section "*Contrast Analysis*" in Methods). These analyses
220 did not reveal any regions that exhibited significantly higher or lower brain activity in
221 the youth compared to others (the combination of young to middle-aged and older
222 adults) (Table 1). Similarly, we did not observe any regions with higher or lower brain
223 activity in older adults compared to others (the combination of the youth and young to
224 middle-aged adults) (Table 1). These results excluded the possibilities of increase/de-
225 crease-then-stable and stable-then-increase/decrease trajectories (Fig. 3, panels D, F, G,

and I). In addition, we failed to observe any region showing lower activity in young to middle-aged adults than others (the combination of the youth and older adults), and thereby ruled out the possibility of the upright U-shaped trajectory (Table 1, Fig. 3E).

[Fig. 3]

However, we identified greater activity in young to middle-aged adults compared to others in the frontoparietal regions, including bilateral inferior frontal gyrus and bilateral inferior parietal lobule; the cingulo-opercular regions, including left supplementary motor area, left insula, and right middle cingulate cortex; and a subcortical region—right caudate nucleus (Fig. 4 and Table 1). This result essentially supports an inverted U-shaped trajectory. Notably, none of the clusters showed significant publication bias based on Egger's test (ps > 0.79), and they all showed low between-study heterogeneity (τs < 0.17, Qs < 12.21, I^2s < 25%). This indicates that the observed results are not likely influenced by biased reporting or substantial variability in the included studies. Consistently, further contrast analyses revealed that the young to middle-aged adults showed greater activity than both the youth (Supplementary Fig. S6) and the elderly (Supplementary Fig. S7).

Fitting the Lifespan Trajectories with the GAM

For each region identified from the contrast between young to middle-aged adults and others, the GAM could fit the data significantly with a smooth curve (Fig. 4), with

degrees of freedom varying from 2.9 to 6.7. Peak ages of the inverted U-shaped trajectories were between 24.5 and 39.4 years. Detailed statistics are shown in Supplementary Table S4.

Model Simplification of the Lifespan Trajectories

Considering the GAM may overfit the data, we fitted the results with simpler models commonly adopted in lifespan developmental literature[46-48], including the quadratic, cubic, square root and quadratic logarithmic models, and estimated the goodness of fit by comparing their Akaike information criterion (AIC) (see section "*Model Simplification and Model Comparison*" in Methods). Results showed that the quadratic model provided the best fit for capturing the age-related changes in left inferior parietal lobule, while the square root model demonstrated the best goodness of fit for all the other regions (Supplementary Table S5). We also calculated the peak age for each region based on the optimal model, and results showed that the peak ages ranged from 33.3 to 40.0 years. In addition, we found the peak ages obtained from the above optimal model (i.e., square root or quadratic models) and the GAM are consistent, $r = 0.71$, $p = 0.032$, 95% CI = [0.09 0.93]. See Fig. 4 and Supplementary Table S6 for details.

[Fig. 4]

Fitting the Whole Brain with Square Root and Linear Models

Based on model comparisons, we found that the square root model provided the best

goodness of fit for the age-related change of the brain activities. To supplement the inverted U-shaped results from the contrast analysis, the square root function was then submitted to whole-brain meta-regression analyses in SDM-PSI (see section "*Meta-regression Analyses*" in Methods).

By fitting the activation over the whole brain, we found seven significant brain regions, including the bilateral inferior frontal gyrus, right angular, left inferior parietal lobule, right insula, right caudate nucleus, and left anterior thalamic projections (Fig. 5A and Supplementary Table S7). These results further supported the existence of the inverted U-shaped regions we initially identified (Fig. 4).

In addition, we explored the whole-brain trajectories with a linear meta-regression (see section "*Meta-regression Analyses*" in Methods). However, no significant regions were observed (Fig. 5B), even under a more tolerant threshold of uncorrected $p < 0.01$.

[Fig. 5]

Dissociated Brain Networks with Distinct Lifespan Trajectories

We note that the inverted U-shaped regions constitute only part of the cognitive control-related regions (Fig. 2), and the remaining regions show a less clear trajectory. To further elucidate the spatial distribution of brain regions following these different trajectory patterns, we used the results from the mean SDM analysis (Fig. 1B) as the mask and replotted the results of the contrast analysis between young to middle-aged adults and others with two different thresholds, and then compared them with the Yeo's 7-

network atlas[49] (Fig. 6). Visualization of the spatial distribution patterns revealed a dissociation between the middle frontal gyrus and its adjacent rostral and caudal areas (Fig. 6A). Moreover, the distribution of inverted U-shaped regions was more consistent with the frontoparietal control network (FPCN), and the distribution of non-U-shaped regions was more closely related to the dorsal attention network (DAN, Fig. 6B). The count of voxels revealed that a numerically larger portion of the inverted U-shaped regions overlapped with the FPCN (2,538 voxels) than with the DAN (932 voxels), while the overlap with the cingulo-opercular network (CON) was in between (1,867 voxels). Conversely, a numerically larger portion of the non-U-shaped regions overlapped with the DAN (3,009 voxels) than with the FPN (2,447 voxels), while the overlap with the CON was lower (1,594 voxels).

[Fig. 6]

To further investigate the potential functional difference between the two sets of brain regions, we decoded the related terms with the Neurosynth decoder[41] (see section "*Neurosynth Decoding Analysis*" in Methods). Results showed that the inverted U-shaped regions were related to the term "cognitive control"(r = 0.187), but were less so to "attentional" (r = 0.100) and "monitoring" (r = 0.072). Note the keyword "monitoring" refers to the major function of the cingulo-opercular network[21]. On the other hand, the non-U-shaped regions were related to the term "attentional" (r = 0.240) but were less so to "monitoring" (r = 0.090) and "control" (r = 0.062) (Supplementary Table S8).

This result suggests that the inverted U-shaped and non-U-shaped regions may be associated with cognitive control and attention, respectively, which is consistent with the frontoparietal control network and dorsal attention network as identified in the atlas overlapping analysis.

Lifespan Trajectory of the Laterality

We also tested how the laterality of the brain activity changes with age (see section "*Laterality Analysis*" in Methods). We first modeled the laterality trajectory using the GAM. Results showed a significant model fitting, $F(3.0, 3.7) = 3.49$, $p = 0.012$, $R^2 = 0.24$. Moreover, we fitted the data with the four simplified models (i.e., the quadratic, cubic, square root, and quadratic logarithmic models). The results showed that a square root function provided the best goodness of fit, with the $\beta_{sqrt(age)} = -0.68$ (95% CI = [−1.02, −0.33]), $p < 0.001$. The two-line test suggests the hypothetical peaks from both models did not reach significance (Supplementary Note S2). A visually upright U-shaped trajectory indicated the youth and elderly adults tended to be more left-lateralized across the whole brain. A further comparison of the relative levels of laterality across different age groups revealed that both the youth and the elderly groups exhibited greater left lateralization than the young to middle-aged adult group (Supplementary Note S3). This left-lateralized pattern could be illustrated by the brain map estimated with voxel-wise laterality calculation (Fig. 7).

[Fig. 7]

Discussion

The present study yielded three primary findings: 1) Among different possible trajectories, only the inverted U-shaped trajectories were reliably observed across the whole brain; 2) The cognitive control-related brain regions exhibit heterogeneous lifespan trajectories: the frontoparietal control network (such as the inferior frontal gyrus and inferior parietal lobule) follows inverted U-shaped trajectories, peaking between 24 and 40 years, while the dorsal attention network (such as the frontal eye field and superior parietal lobule) demonstrates less clear trajectories with age; 3) The youth and the elderly demonstrate weaker brain activities and a relatively greater extent of left laterality compared to the young to middle-aged adults. These results provide strong evidence for the existence of cognitive control regions exhibiting inverted U-shaped trajectory, and also show the heterogenous lifespan trajectories in different brain regions.

The Inverted U-shaped Trajectory of Brain Activity Related to Cognitive Control

The main finding is that a wide range of cognitive control regions follow inverted U-shaped lifespan trajectories, but no regions showed decrease-then-stable (Fig. 3D), upright U-shaped (Fig. 3E), stable-then-increase (Fig. 3F), increase-then-stable (Fig. 3G), stable-then-decrease (Fig. 3I), or linear trajectories (Fig. 3A and 3C).

The greater activation in the frontoparietal control network among young to middle-aged adults compared to the youth and the elderly supports the notion that cognitive

control abilities may not be fully developed in children and may decline in the elderly. This finding is consistent with the idea that the cognitive control system is most effective in young adulthood, suggesting a possible correlation between the higher functional activations in the brain and the superior performance of young adults on cognitive control tasks[50]. Consistently, a previous study[29] showed that behavioral performance (success of interference suppression) is positively correlated with the activity in frontal regions. Similar patterns have been repeatedly reported[51,52], although the opposite results have also been observed[53].

The inverted U-shaped trajectory of brain activation might be associated with the development of brain structure and functional changes. First, it may reflect the well-documented structural changes that occur in these regions across the lifespan, which include synaptic pruning, myelination, cortical thinning, and white matter maturation[19,54]. For example, the density of dopamine receptors increases during adolescence and young adulthood and subsequently declines with age[55]. These changes can affect the efficiency and connectivity of neural circuits within the frontoparietal control network[13,56]. Second, the inverted U-shaped trajectory may also arise from functional changes resulting from the modulation of neurotransmitters, hormones, and environmental factors[57]. Understanding change patterns of brain structure and function is critical for developing interventions and treatments aimed at improving cognitive control abilities across the lifespan.

The present results further revealed that the inverted U-shaped lifespan trajectories of cognitive control regions are not uniform. The GAM fitting results (Fig. 4, Supplementary Table S4) showed that the subregions exhibited varying degrees of association with age. Moreover, the model simplification demonstrated different underlying trajectory curves, with most regions showing a skewed shape that could best be fitted with a square root model, except that one region showed a symmetric quadratic shape. The quadratic lifespan trajectory has been well-documented in previous studies[19,46,48,58], while the application of the square root model has been relatively rare[59]. The square root model can better capture the early peak in the trajectory. We also identified different peak ages for those regions, ranging from 24 to 40 years, suggesting that cognitive control regions may not develop at the same rate.

Hierarchical development trajectories in different brain networks

Previous research has indicated that the attentional orientation function is preserved during ageing[35,60]. Consistently, we found that the dorsal attention network regions underlying the attentional orientation showed no significant age-related change, in contrast to the inverted U-shaped trajectory in frontoparietal control network regions. In addition, we observed that the supporting regions mediating top-down control with motor[61] (right cerebellum, Fig. 2) and sensory[62] (left anterior thalamic projections, Fig. 2) functions also lack the sensitivity to age. The dissociation across regions may reflect hierarchical associations with age on brain function.

The brain regions are organized in a functional hierarchy, with the frontoparietal control network at the highest level. It acts as a hub that interacts with other systems, including the dorsal attention network[63]. The cingulo-opercular network did not present a clear dissociation of trajectory patterns, possibly suggesting its intermediate position between the frontoparietal control and dorsal attention networks[64]. During conflict tasks, these networks function in a hierarchical manner. The frontoparietal control network maintains task goals and resolves conflicts, the cingulo-opercular network monitors conflict, and the dorsal attention network directs attention towards task-relevant stimuli[65]. Even within the prefrontal cortex itself, a hierarchical organization exists, with middle frontal areas occupying the peak position[66]. This is in line with our finding that the middle frontal cortex is dissociated from rostral and caudal frontal regions (Fig. 6A). In addition, previous research suggests that the frontoparietal control network can be further divided[67], with the rostral and caudal frontal regions observed in our study aligning closely with the sub-network that connects more strongly with the dorsolateral attention network. This may explain why some areas within the frontal region do not show age-related changes.

Furthermore, different brain regions exhibit different age-related changes. Higher-order regions typically have more complex lifespan trajectories[58] and reach peaks during later periods[56,68]. Specifically, prefrontal control regions are among the last to mature and one of the earliest to decline[5,13,69]. Therefore, the different lifespan trajectory

patterns among different networks likely reflect their hierarchical positions of age-related changes.

Implications for the Compensatory and Asymmetry Reduction Theories

Critically, there was no region showing higher activity in the elderly compared to the young to middle-aged adults, but we observed several regions showing the opposite (Supplementary Note S3 and Table S9). The results persisted after we controlled the behavioral congruency effect (Supplementary Note S4 and Fig. S8), thereby ruling out the possibility of weaker brain activity associated with poor behavioral performance in the elderly. The observed decrease in brain activation among the elderly might be attributed to several interrelated factors. First, cognitive control regions, especially the frontal area, tend to shrink with age, leading to a reduction in overall brain volume and potential loss of synaptic integrity[70]. This shrinkage can impair the brain's ability to effectively process and manage complex tasks. Another significant factor is the impairment of neurovascular coupling, the relationship between neuronal activity, synaptic function, and subsequent blood flow, which disrupts the brain's ability to maintain optimal function during cognitive tasks[71,72]. Furthermore, the decrease in cerebral blood flow with age can diminish the delivery of essential nutrients and oxygen to the brain, impairing its overall functionality[73]. These changes could lead to regional abnormalities, such as blood flow, blood volume, metabolic rate, or BOLD-derived physiologic

422 proxies like the fractional amplitude of low-frequency fluctuation and regional homo-
423 geneity[74]. Future studies may validate and extend our study by adopting the age-sensi-
424 tive regions we observed and testing other measurements, such as resting-state data,
425 which are more easily collected in large-scale studies involving children and the elderly
426 compared to task-based activations.

427 The compensatory theory[10] proposes that the elderly recruit additional brain re-
428 gions to compensate for age-related cognitive decline, but our results did not show this
429 pattern. We suggest that the absence of compensatory upregulation in frontoparietal
430 regions among the elderly observed in our study might be attributed to limited available
431 resources when cognitive control related brain regions are already fully engaged[75,76].
432 Previous research has shown that younger adults recruit lower activity in frontoparietal
433 regions during the congruent condition but significantly greater activities during the
434 incongruent condition. In contrast, older adults already show a relatively higher activa-
435 tion during the congruent condition, leaving limited capacity for further increases in
436 activation during the incongruent condition[32]. This is consistent with our findings,
437 which are based on the contrast between incongruent and congruent conditions.
438 Moreover, the nature of the task investigated might influence whether there is an up-
439 regulation in cognitive control regions with age. Upregulation in the frontal regions
440 usually compensates for memory and sensory declination due to deficits in the hippo-
441 campus and sensory cortices[77]. Semantic cognition[78] might also be a target of compen-

sation. However, conflict tasks seem to rely minimally on memory, and involve relatively simple sensory stimuli (e.g., colors and locations) and simple semantic processing (e.g., reading a word). As such, conflict tasks may not necessitate compensation in these functions.

In addition, compensation in older adults may manifest as increased recruitment of bilateral regions and homologues with age[79]. For example, the hemispheric asymmetry reduction in older adults (HAROLD) theory[80] suggests that older adults typically exhibit less lateralization, either as a compensatory response to functional deficits or as a reflection of neural dedifferentiation. However, we observed that the elderly showed greater left lateralization compared to young to middle-aged adults. This finding is inconsistent with the assumption of HAROLD but aligns with the right hemi-ageing model[81], which posits that the right hemisphere is more vulnerable to age-related decline. Prior research has shown that functional connectivity within the frontoparietal control network is more disrupted in the right hemisphere than in the left during ageing[82]. This suggests that neural resources in the right hemisphere might be more limited for the elderly, reducing its capacity to compensate for cognitive demands. Stronger patterns of left laterality were also identified in childhood in the current study, primarily noticeable within the prefrontal region (Fig. 7), which may reflect the earlier development of the left hemisphere compared to the right[83]. In contrast, we found lower lateralization in young adults. It is possible that previous studies showing stronger laterality in young adults may have been biased by too small sample sizes and the use of non-

463 quantitative methods for calculation of laterality[84,85]. Moreover, because both left and
464 right lateralized results were reported in the literature on laterality[81], it is reasonable to
465 observe low laterality for young to middle-aged adults in the current meta-analysis.

466 **Methodology Implications**

467 By incorporating all the studies, our results demonstrate that the SDM can reliably iden-
468 tify brain regions as the ALE. However, the SDM has the added advantage of fully
469 utilizing existing effect size data and coordinates[86], allowing us to compare the relative
470 activity strength among various age groups, such as the contrast between young to mid-
471 dle-aged adults and elderly groups. More importantly, this approach allows for meta-
472 regressions to examine parametric relationships between brain region activity and age,
473 providing insights into the lifespan trajectories of cognitive control regions.

474 **Limitation of Results**

475 One caveat to consider in this study is the non-uniform distribution of age among the
476 included studies. Specifically, there is a noticeable gap in the age range of 45 to 60
477 years. Consequently, the observed age distribution could potentially influence the re-
478 sults of the regression analysis. We hope that future research could allocate more atten-
479 tion to the middle-aged period, considering the significant cognitive and neural changes
480 during this stage, such as the onset of cognitive decline[15,17,87]. In addition, it is crucial
481 to avoid the occurrence of ecological fallacy[88] (associations observed at the group level

are erroneously assumed to apply to individuals) when interpreting the results of meta-regression analyses. Therefore, associations between brain activities and age across various studies do not provide direct insights into the specific age-related changes at the individual level. Future research incorporating individual-level investigations (e.g., longitudinal follow-up studies) is crucial to obtaining a more comprehensive understanding of these relationships.

Conclusions

Our meta-analysis adopted advanced meta-regression approaches to chart the lifespan trajectories of cognitive control brain activities. We observed inverted U-shaped changing patterns in regions aligned with the frontoparietal control network, with the peaks occurring between 24 and 40 years. In contrast, the dorsal attention network does not present a clear age-related trajectory. This dissociation may reflect the hierarchy of brain development in different regions. No other trajectory patterns were observed, highlighting the predominance of the inverted U-shaped pattern in the lifespan trajectory of cognitive control. Furthermore, we found the youth and elderly showed a more asymmetric brain distribution than young to middle-aged adults. In sum, these results demonstrate the multifaceted nature of age-related changes in cognitive control brain function.

Methods

Literature Preparation

Literature Search

We report how we determined all data exclusions (if any), all manipulations, and all measures in the study. We first searched both English and Chinese articles on the youth and the elderly from PUBMED, Web of Science and CNKI (China National Knowledge Infrastructure) till 2022. The following search terms were applied in titles, abstracts, table of contents, indexing, and key concepts: *("Stroop" OR "Flanker" OR "Simon" OR "SNARC" OR "Navon" OR "interference" OR "cognitive conflict") AND ("fMRI" OR "functional resonance imaging" OR "functional imaging" OR "neuroimaging" OR "PET") AND ("children" OR "kids" OR "adolescents" OR "teenagers" OR "underage" OR "aged" OR "old" OR "older" OR "elder" OR "elderly" OR "senior" OR "development" OR "developmental" OR "aging" OR "life span").* The above process yielded 3,484 articles. In addition, 111 studies on young to middle-aged adults from a previous meta-analysis study[21] were included in the literature pool, 40 of which were excluded according to the current literature exclusion criteria (see below). Moreover, we screened 16 articles citing or being cited by the crucial literature. After removing duplicates, the literature search identified 2,930 articles.

Exclusion Criteria

We excluded any articles that met one or more of the following predefined exclusion criteria[89]: 1) not in English or Chinese; 2) not including healthy human participants; 3) case study; 4) not empirical study; 5) not functional resonance imaging (fMRI) or positron emission tomography (PET) study; 6) not whole-brain results (i.e., not have covered the whole gray matter); 7) not in Talairach or Montreal Neurological Institute (MNI) space; 8) not reflecting the congruency effect (i.e., contrasts between incongruent and congruent or between incongruent and neutral conditions); 9) not reporting exact mean age of participants.

A total of 119 articles were identified as eligible for inclusion in our meta-analyses. No statistical methods were used to pre-determine sample sizes, but our sample sizes are similar to or larger than those reported in previous publications[31,90]. Supplementary Fig. S1 shows the preferred reporting items for systematic reviews and meta-analyses (PRISMA)[91] flow chart for the literature screening process. The 119 articles included 129 studies (individual contrasts reported in the articles) with 3,388 participants and 1,579 activation foci reported. All studies were published or completed between 1994 and 2022. None of the experiments share the same group of participants. The included studies are written in English (124 studies) and Chinese (5 studies). Of the studies included, 125 were published in peer-reviewed journals, and 4 were master's theses. All included studies reported the task type used, including 74 studies utilizing Stroop-like

task (57%), 25 studies utilizing Simon task (19%), 25 studies utilizing Flanker task (19%), 2 studies utilizing a combination of Simon and Flanker tasks (2%), 1 study utilizing a combination of Simon and Stroop tasks (1%), and 3 studies utilizing multi-source interference task (2%). In addition, the contrasts conducted to reveal brain activations were also reported, with 98 studies (76%) resulting from the contrast of Incongruent trials > Congruent trials, 25 studies (19%) resulting from the contrast of Incongruent trials > Neutral trials, and 6 studies (5%) resulting from the union contrast of Incongruent trials > Congruent trials and Incongruent trials > Neutral trials. Regarding the handedness of participants in the included studies, 89 studies (69%) included right-handed participants only, 6 studies (5%) included both left and right-handed participants, while 34 studies (26%) did not report this information. Furthermore, 78 studies (60%) included only correct response trials, 2 studies (2%) included both correct and incorrect response trials, while 49 studies (38%) did not report this information. A detailed description of these features for each study is available in the Supplementary Table S1. To eliminate the influence of these confounding factors, we included them as covariates in the modeling analyses.

Coding Procedure

A coding manual was formulated to record pertinent study information, including authors, publication dates, experimental tasks, contrasts, and sample demographics (such

as the average age and sample size). To ensure coding accuracy, two authors independently coded all studies, with discrepancies resolved through discussion or reference to the original studies. In instances where studies lacked essential information, such as peak coordinates for relevant contrasts, participant age averages, or data for specific age groups, efforts were made to contact the authors via e-mail to obtain the relevant data. In addition, both coordinates and effect sizes (i.e., Hedge's *g*) were extracted from each study. Further, Talairach space coordinates were transformed to MNI coordinates using the Lancaster transform[92].

Meta-Analytic Procedure

Activation Likelihood Estimation (ALE)

In order to obtain a comprehensive understanding of cognitive control-related brain activity across all age groups and to replicate a prior study[21], we initially conducted a single dataset meta-analysis using BrainMap GingerALE software[93] (version 3.0.2, http://www.brainmap.org). This meta-analytical approach, known as activation likelihood estimation, utilizes the spatial convergence of brain activity across multiple studies to determine the probability of activation in specific regions. Foci from individual studies were transformed into a standardized coordinate space and modeled as Gaussian probability values that accounted for variability in the number of participants in each

study. In situations where foci overlapped across studies, multiple Gaussians were associated with a single focus, and ALE selected the Gaussian with maximum probability for each focus[93]. Subsequently, ALE score maps were generated by comparing these modeled Gaussian distributions with a null distribution that simulated random brain effects. The null distribution was generated using the same sample size and number of foci groups as the experimental dataset for 1,000 times[94]. ALE scores were then used to calculate *p*-values, which were based on the proportion of values higher than a certain threshold in the null distribution. This resulted in a statistical ALE map that differentiated true brain effects from random effects. A cluster-defining threshold of $p < 0.001$ and a minimum cluster size of 10 voxels (80 mm^3) were utilized to compute ALE maps, consistent with the threshold applied in the seed-based *d* mapping (SDM) approach (see below).

Seed-based *d* (Effect Size) Mapping

SDM is an alternative approach to statistically synthesize results from multiple neuroimaging experiments[86]. Similar to ALE, SDM employs a coordinate-based random-effect approach to amalgamate peak coordinate information into a standard space across several experiments. However, while ALE solely considers the binary feature (i.e., active versus inactive) of peak coordinates, SDM takes into account the quantitative effect size (can be positive or negative) connected to each peak and reconstructs the initial

parametric maps of individual experiments before amalgamating them into a meta-analytic map[95]. Therefore, the use of a distinct algorithm in SDM from ALE allows us to scrutinize the robustness and replicability of the outcomes obtained via ALE. More importantly, SDM enables the inclusion of covariates in the meta-regression analyses to reflect the changes in brain function across the lifespan.

We conducted three types of analyses using the SDM approach. Firstly, we estimated the mean activation across all age groups and compared the results with ALE's single dataset meta-analysis results. Secondly, we conducted contrasts between two groups of studies (e.g., between young to middle-aged adults and a combination of the youth and elderly groups) to identify brain regions that showed different levels of activity across age. This analysis method served to investigate the hypothesized lifespan trajectories, such as the inverted U-shaped pattern by elucidating neural activity variations linked to age. Thirdly, we defined specific models (e.g., linear and square root models) to fit the whole brain to validate brain regions adhering to the hypothetical lifespan changing patterns. This type of analysis aimed to explore various lifespan trajectories, recognizing that different brain regions might follow distinct model functions. See below for the details.

These analyses were conducted using the software of SDM with permutation of subject images (SDM-PSI) (version 6.22, https://www.sdmproject.com). Effect size maps were built for the 129 individual experiments. This was accomplished by (a) converting the statistical value of each peak coordinate into an estimate of effect size

(Hedge's *g*) using standard formulas[96] and (b) convolving these peaks with a fully anisotropic unnormalized Gaussian kernel ($\alpha = 1$, FWHM = 20 mm) within the boundaries of a gray matter template (voxel size = 2×2×2 mm^3). Imputation (50 times) was conducted for each study separately to obtain a reliable estimate of brain activation maps[95]. In addition, the individual effect size maps were combined using a random-effect general linear model. To assess the statistical significance of activations in the resulting meta-analytic effect size map, 1,000 random permutations of activation peaks within the gray matter template were compared. Finally, the meta-analytic maps were thresholded using a voxel-wise family-wise error (FWE) corrected threshold of $p < 0.001$ and a cluster-wise extent threshold of 10 voxels[97].

Mean Analyses Across all Studies

This analysis aimed to characterize the activation distributions of cognitive control-related brain regions across all studies, which was conducted utilizing the "Mean" function in SDM-PSI software. In order to verify the reliability of the SDM analysis results, we compared the results with the single dataset meta-analysis using ALE. Results from this analysis were further used as regions of interest (ROIs) in the subsequent model fitting analyses (see section "*Generalized Additive Model (GAM) Fitting*" below). The possibility of publication bias for resultant clusters was examined using Egger's test[98], in which any result showing $p < 0.05$ was regarded as having significant publication bias. Heterogeneity was evaluated using the I^2 index, which quantifies the proportion

635 of total variability attributable to heterogeneity between studies. A value less than 25%
636 indicates low heterogeneity among the included studies[99].

637 *Contrast Analyses*

638 To test our hypothesis that cognitive control related brain activities follow an inverted
639 U-shaped trajectory with age, we categorized each study based on the mean age of par-
640 ticipants into youth (< 18 years), young to middle-aged adults (18−59 years), and el-
641 derly (>= 60 years) groups. The age boundaries were determined to minimize age dis-
642 tribution overlap. We utilized SDM-PSI to perform a contrast analysis between the
643 group of young to middle-aged adults and the combination of other groups in order to
644 examine whether there are brain regions that exhibit an inverted U-shaped lifespan tra-
645 jectory. This was achieved by assigning studies from the young to middle-aged adult
646 group as 1 and all other studies as −1. This analysis yielded two results, one showing
647 higher activity in young to middle-aged adults than the youth and elderly groups, and
648 the other showing the opposite. Like the mean analysis, results from this analysis were
649 used as ROIs in the subsequent model fitting analyses (see sections “Generalized Ad-
650 ditive Model (GAM) Fitting” and “Model Simplification and Model Comparison”).

651 In addition, to explore other possible trajectories, such as the increase-and-stable
652 pattern[5], we conducted contrast analyses between the youth and the combined group of
653 young to middle-aged and the elderly, as well as between the elderly and the combined

group of youth and young to middle-aged adults. Furthermore, to address the controversies in previous studies, we conducted contrast analyses between older and young to middle-aged adult groups, and between the youth and young to middle-aged adult groups, respectively.

Meta-regression Analyses

To better describe the possible lifespan trajectories of the whole brain, we carried out meta-regression analyses with the age and/or its derivatives as regressors. Two regressions were conducted across the whole-brain, including a linear regression (with only age as the regressor) and a square root regression (with age and its square root as separate regressors). The linear regression aimed to test regions with increasing/decreasing activity with age, and the square root regression aimed to test regions with the inverted U-shaped trajectories based on the model fitting analyses (see below).

Data Extraction

Masks were generated for each ROI derived from the mean and contrast analyses in SDM-PSI as described above. Subsequently, we extracted the effect sizes for each mask. Fifty values were obtained from the SDM iterations and subsequently averaged for each study in each region. The iterated variances were also averaged in a similar way. Additionally, we removed the outliers (beyond 3 standard deviations from the mean) in the following model fitting analyses.

673 **Generalized Additive Model (GAM) Fitting**

674 To precisely estimate the inverted U-shaped trajectories, we adopted the GAM to fit the
675 curves. The GAM allows for flexible, nonparametric smoothing of predictor varia-
676 bles[100], and has been widely used to depict the lifespan trajectories[101,102]. We imple-
677 mented GAMs using the "mgcv" package[100] in R. For each ROI, we fitted a GAM with
678 the following formula:

679 $$g \sim s(age) + covariates,$$

680 where g is the effect size (dependent variable), s(age) represents a smoothing spline of
681 age (predictor variable), and covariates represent the dummy-coded categorical covari-
682 ate regressors. These regressors correspond to six aspects of the included studies: (1)
683 the presence of various conflict types (e.g., Stroop or Simon), (2) the mixed subject
684 samples based on handedness (e.g., right handed only or both handed), (3) the different
685 contrasts in reporting congruency effects (e.g., incongruent – congruent or incongruent
686 – neutral), (4) different trial types regarding whether they excluded error trials, (5) the
687 use of different types of experimental design (i.e., event-related or block designs), and
688 (6) the behavioral congruency effects measured by reaction time. Notably, we adopted
689 median imputation[103] for 9 studies (accounting for 6.98% of the total included studies)
690 not reporting the behavioral congruency effects, and included an indicator regressor to
691 account for the potential impact of imputation[104]. The validity of this imputation ap-

proach was confirmed through a robustness analysis (Supplementary Note S4). We incorporated these covariates to control for their potential confounding effects related to age, which could otherwise influence our results. We also adjusted the estimate with a weight parameter, which was the reciprocal of variance. We used penalized regression splines, with the amount of smoothing determined automatically based on generalized cross validation.

For each ROI, we quantified the peak age by choosing the highest prediction of a fine-grained age scale (1,000 points from 8 to 74 years old). We also calculated the estimated degree of freedom (EDF) for the smooth curve by summing up the degree of freedom for each penalized term (i.e., s(age).1 to s(age).9).

Model Simplification and Model Comparison

While the GAM analysis may yield good fitting results on the data, it is important to acknowledge its potential limitations. One concern is that it can fit the data with high degree of freedoms (up to 7.0, Supplementary Table S4), which makes it susceptible to over-fitting and harder to generalize. Another issue is its poor interpretability. Therefore, we next sought to fit the data with simpler models.

To this end, we used the "metafor" package in R to fit these effect sizes with the age and its derivatives as predictors. Specifically, we tested four non-linear models (see below formulas and Fig. 3). Quadratic and cubic models were included based on previous studies[46,47]; quadratic logarithmic and square-root models were included to capture

712 the possible skewed trajectory, which would reflect the asymmetric trajectory of devel-
713 opment and decline of cognitive control[5]. Each model was fitted to each ROI separately.
714 In addition, we included the same covariates as the GAM analysis in each regression
715 model. We calculated the Akaike information criterion (AIC) to evaluate the goodness
716 of fit for each model.

717 1) Quadratic model

718 $g \sim \text{age} + \text{age}^2 + \text{covariates}$

719 2) Cubic model

720 $g \sim \text{age} + \text{age}^2 + \text{age}^3 + \text{covariates}$

721 3) Quadratic logarithmic model

722 $g \sim \log(\text{age}) + (\log(\text{age}))^2 + \text{covariates}$

723 4) Square root model

724 $g \sim \text{age} + \text{sqrt}(\text{age}) + \text{covariates}$

725 **Neurosynth Decoding Analysis**

726 To investigate the potential functional difference between the two sets of brain regions
727 reported in section "*Dissociated Brain Networks with Distinct Lifespan Trajectories*"
728 of Results, we generated two binary maps from the contrast analysis between young to
729 middle-aged adults and the combination of other groups, and then submitted them to
730 the Neurosynth decoding system[41]. As the non-U-shaped map is defined as the converse
731 of the inverted U-shaped map, they were obtained by applying thresholds of $0.1 < p <$

732 0.9 and $p < 0.05$, respectively. These lenient threshold boundaries were used to mini-
733 mize the influence of sparsity on the decoding results. The two-boundary threshold was
734 used in generating the non-U-shaped map, as the original statistical map from the SDM-
735 PSI analysis was one-tailed, which means the threshold of $p > 0.9$ indicates the upright
736 U-shaped trend instead of a non-U-shaped trajectory. Additionally, to focus on the brain
737 regions specifically related to cognitive control, the two maps were masked by using
738 results from the mean SDM analysis (Fig. 1B). In the decoding results, we deleted terms
739 that were related to brain regions (e.g., "frontal"), not functional specific (e.g., "task"),
740 and duplicated (e.g., "attention" was removed if there was already "attentional").

741 **Laterality Analysis**

742 We calculated the laterality based on the effect size of reported brain coordinates from
743 each study. We computed the sum of effect sizes across coordinates for the left and right
744 hemisphere, respectively, yielding one global effect size each (i.e., g_L and g_R). Then,
745 we calculated the index of brain laterality with the following equation[105]:

746 $$\text{laterality} = \frac{g_L - g_R}{g_L + g_R},$$

747 which was then submitted to the GAM and simplified models (i.e., the quadratic, cubic,
748 square root, and quadratic logarithmic models).

749 To illustrate the contribution of different brain regions to the age-related change
750 of laterality, we calculated the laterality for each voxel[78]. We first used the SDM-PSI

751 to conduct a mean analysis for each age group (i.e., the youth, young to middle-aged
752 adult and elderly), yielding three z-maps. Then the laterality was computed with the
753 above equation for each voxel from the left hemisphere. The opposite values were cal-
754 culated for the right hemisphere. To avoid the bias due to asymmetric brain hemispheres,
755 we removed voxels without corresponding mirror coordinates. The results were visual-
756 ized confining to the brain regions estimated from the grand mean analyses (Fig. 1B).

Data Availability

The meta-data that support the findings of this study are available in Zenodo with the identifier doi: 10.5281/zenodo.12727621[106].

Code Availability

All codes conducting the ROI analyses are available in Zenodo with the identifier doi: 10.5281/zenodo.12727621[106].

Acknowledgement

We thank Fergus I.M. Craik, Beatriz Luna, and Haiyan Wu for valuable suggestions on this manuscript. We also thank Jing Yang and Yifan Zhang for the data check of extracted coordinates. Z.L. discloses support for the research of this work from Scientific Research Fund of Zhejiang Provincial Education Department (Y202249966), Starting Research Fund from Hangzhou Normal University (2021QDL079), and STI 2030-Major Projects (2021ZD0201705). I.T.P discloses support for the research of this work from the Eunice Kennedy Shriver National Institute of Child Health and Human Development (NICHD) (HD098235). G.Y. discloses support for the research of this work from Jiefeng Jiang, and China Postdoctoral Science Foundation (2019M650884). X.L. discloses support for the research of this work from the Ministry of Science and Technology of the People's Republic of China (2021ZD0200505). The funders had no role in study design, data collection and analysis, decision to publish or preparation of the manuscript.

Author Contributions Statement

Conceptualization: Z.L. and G.Y.; Methodology: G.Y.; Formal analysis: G.Y. and Z.L. ; Data curation: Z.L.; Writing original draft: G.Y. and Z.L.; Writing, review, and editing: G.Y., Z.L., I.T.P., L.W., X.L. and J.R.; Funding: Z.L., I.T.P., X.L. and G.Y; Supervision: G.Y.

Competing Interests Statement

The authors declare no competing interests.

Inclusion & Ethics

All collaborators of this study fulfilled the criteria for authorship required by Nature Portfolio journals have been included as authors, as their participation was essential for implementation of the study and improvement of the manuscript. Roles and responsibilities were agreed among collaborators ahead of the research. This work does not include findings that are locally relevant. As a meta-analysis, this study does not involve direct interactions with human participants or the collection of new data. Each of the original studies included in this meta-analysis obtained ethical approval from their respective institutions, and we confirm that we complied with all applicable ethical guidelines and regulations.

Tables

Table 1. Brain areas activated in the contrast of one age group versus others (voxel-wise FWE-corrected, $p < 0.001$, with minimum cluster size ≥ 10 voxels) with the SDM-PSI.

Order	# Voxels	*Z*	*p*	L/R	MNI coordinate			Anatomical location	BA
					x	y	z		
Young to middle-aged adults > Others									
1	1165	4.713	< 0.001	R	52	16	4	inferior frontal gyrus	48
2	607	4.895	< 0.001	L	−46	16	26	inferior frontal gyrus	48
3	569	4.289	< 0.001	R	54	−48	42	inferior parietal lobule	40
4	215	3.405	< 0.001	L	−8	0	58	supplementary motor area	6
5	202	3.830	< 0.001	L	−36	−54	42	inferior parietal lobule	40
6	106	3.245	< 0.001	R	10	4	6	caudate nucleus	/
7	76	3.231	< 0.001	L	−38	24	0	insula	47
8	33	3.119	< 0.001	L	−36	12	−6	insula	48
9	10	2.794	< 0.001	R	4	−16	44	middle cingulate cortex	23
Young to middle-aged adults < Others									
None									
The youth > Others									
None									
The youth < Others									
None									
The elderly > Others									
None									
The elderly < Others									
None									

Note. The brain regions in the table correspond to the regions in Fig. 4. MNI = Montreal Neurological Institute, BA = Brodmann area, L = left, R = right.

Figure Legends/Captions

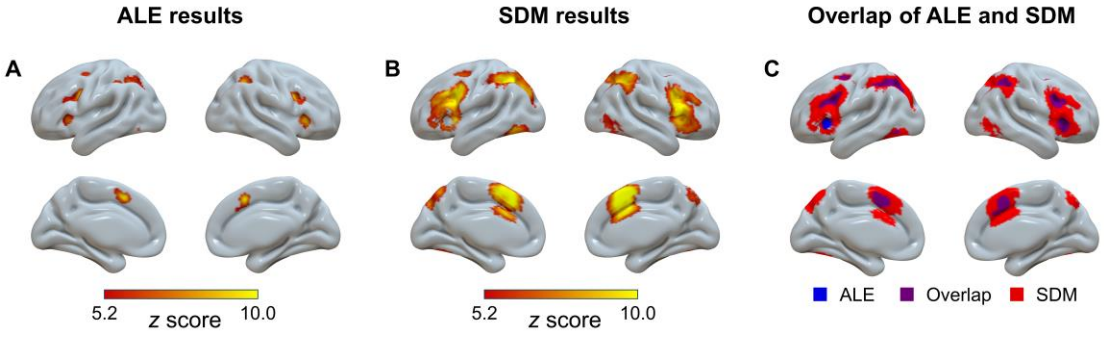

Fig. 1. Overview of significant clusters across all studies regardless of age in the ALE meta-analysis (A), the SDM meta-analysis (B), and their overlap (C). ALE = activation likelihood estimation; SDM = seed-based *d* mapping.

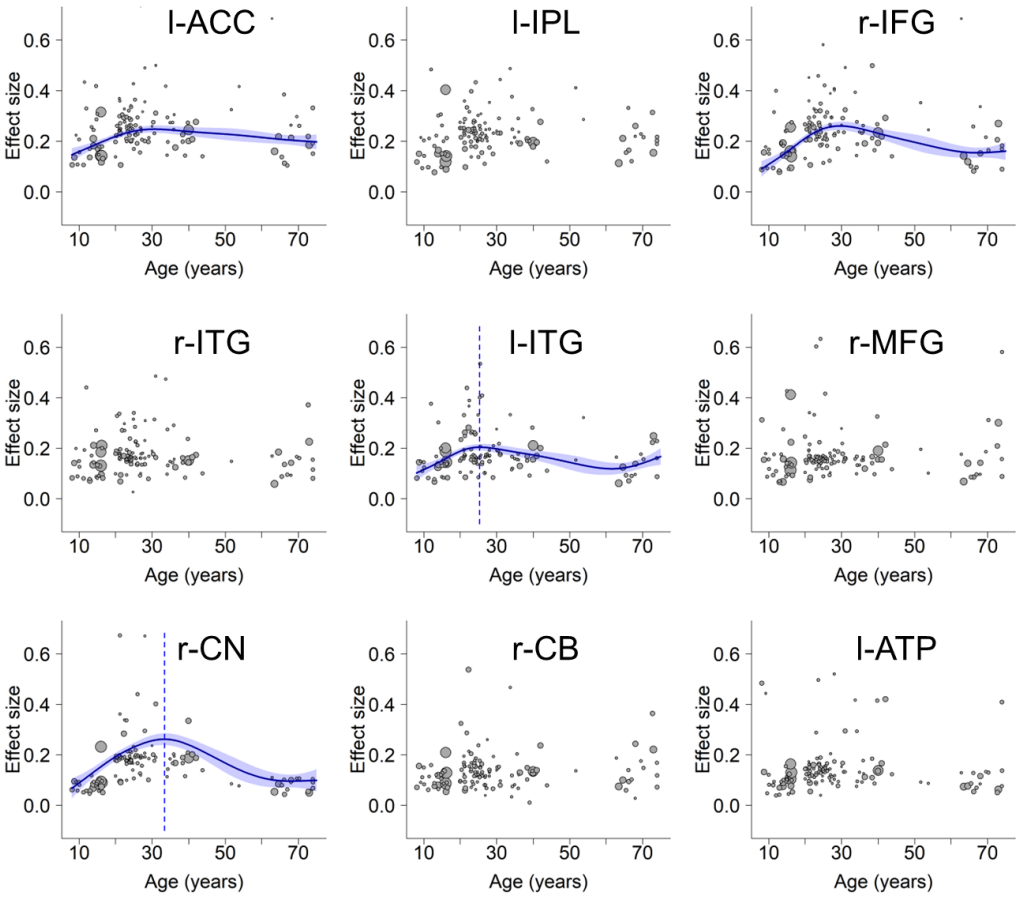

Fig. 2. Lifespan trajectories within regions identified in the mean analysis. l-ACC: left anterior cingulate cortex, l-IPL: left inferior parietal lobule, r-IFG: right inferior frontal gyrus, r-ITG: right inferior temporal gyrus, l-ITG: left inferior temporal gyrus, r-MFG: right middle frontal gyrus, r-CN: right caudate nucleus, r-CB: right cerebellum, l-ATP: left anterior thalamic projections. Scattered plots are the effect sizes as a function of age, with curves fitted by GAM. The sizes of the scattered dots show the square root of model weights (1/variance) for each study. Shaded areas around the curves represent standard errors. Dashed lines indicate peak ages. Panels l-ACC and l-IPL do not show the peak age due to an insignificant decrease at the later stage (Supplementary Note S2).

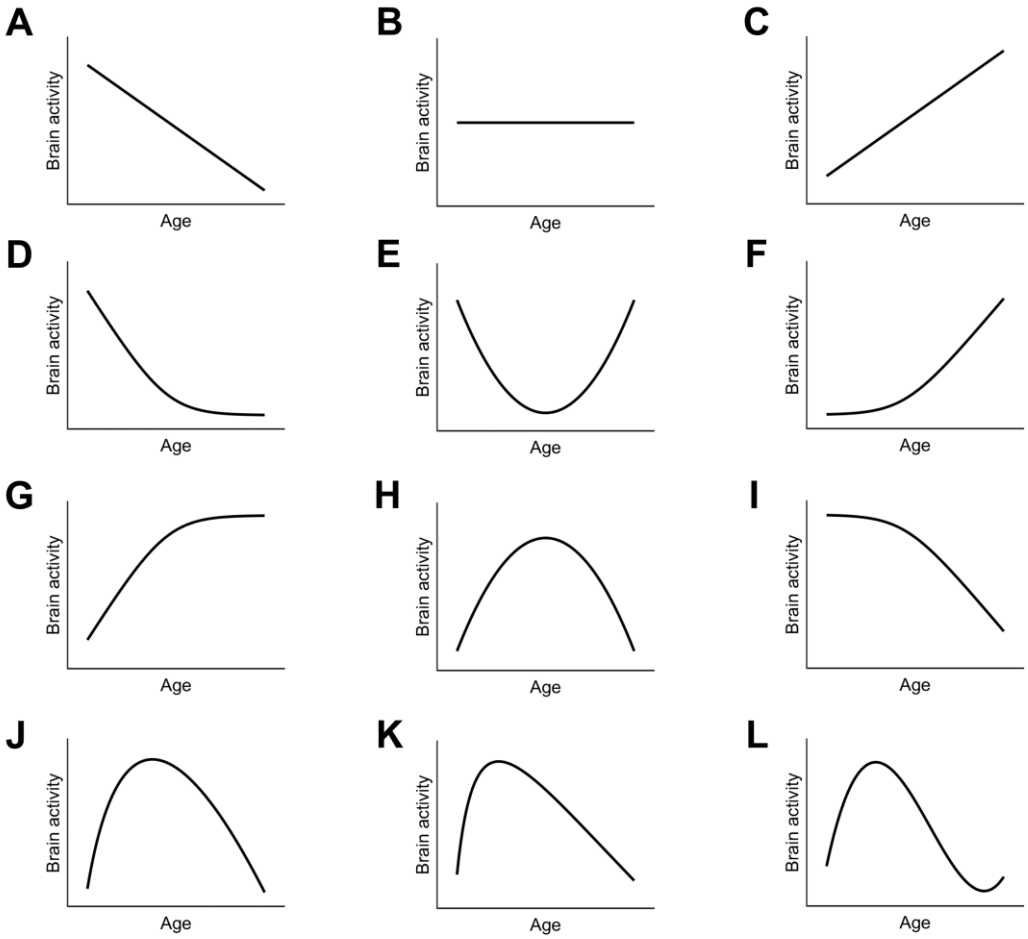

Fig. 3. The lifespan trajectories explored in our study. Panels A-C show linear decrease, flat, and linear increase patterns, respectively, and were modelled with the linear function. Panels E and H show the upright and inverted U-shapes, respectively, and were tested with the contrast between young to middle-aged adults and others, as well as with the quadratic function. Panels D, F, G, and I show combinations of a stable period and an increase/decrease period across the lifespan, and were tested with the contrast between the youth and others, or between the elderly and others. Panels J, K and L show the variants of inverted U-shaped trajectories, which capture the possibly early peak feature. They were tested with square root, quadratic logarithmic, and cubic functions, respectively. See Methods for detailed models.

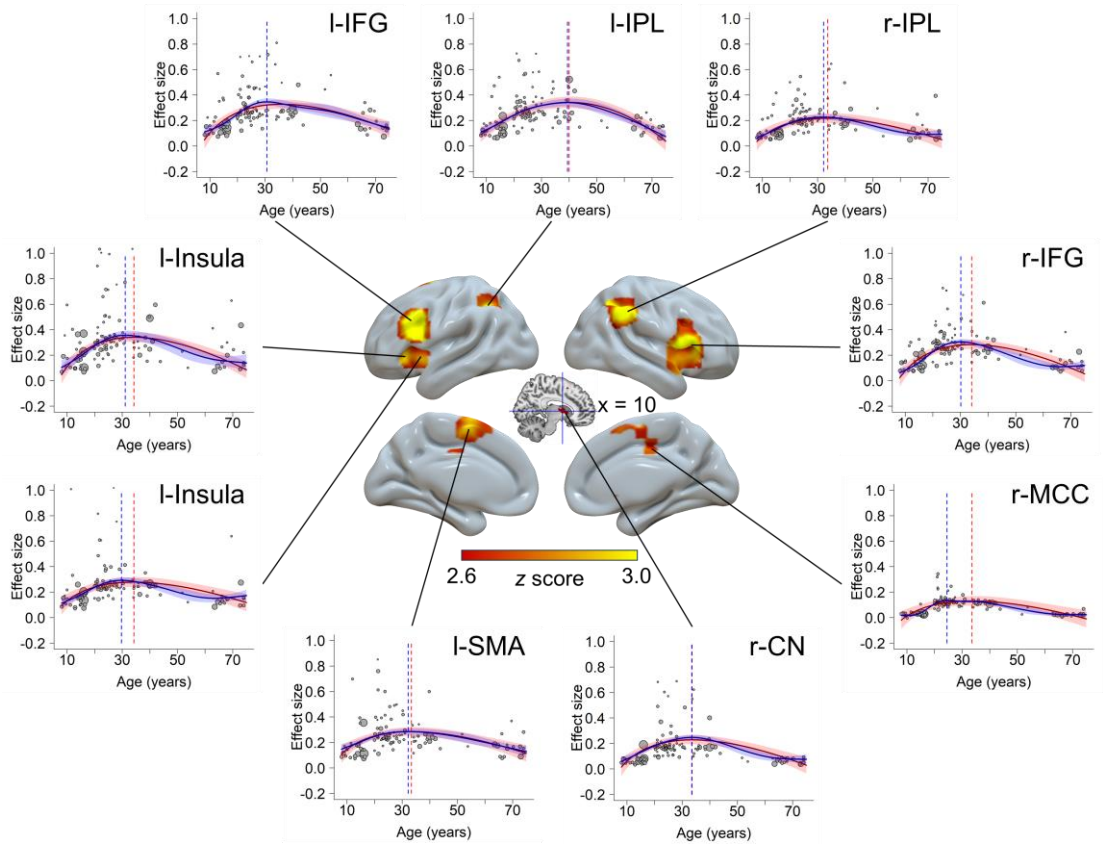

Fig. 4. Brain regions showing inverted U-shaped trajectory patterns. Scattered plots are the effect size as a function of age, with curves fitted by GAM (blue color) and the best simplified model (red color). Shaded areas around the curves represent standard errors. Dashed vertical lines show peak ages estimated from GAM (blue) and simplified model (red). The sizes of the scattered dots show the square root of model weights (1/variance) for each study. r-IFG: right inferior frontal gyrus, l-IFG: left inferior frontal gyrus, r-IPL: right inferior parietal lobule, l-SMA: left supplementary motor area, l-IPL: left inferior parietal lobule, r-CN: right caudate nucleus, l-Insula: left insula, r-MCC: right middle cingulate cortex.

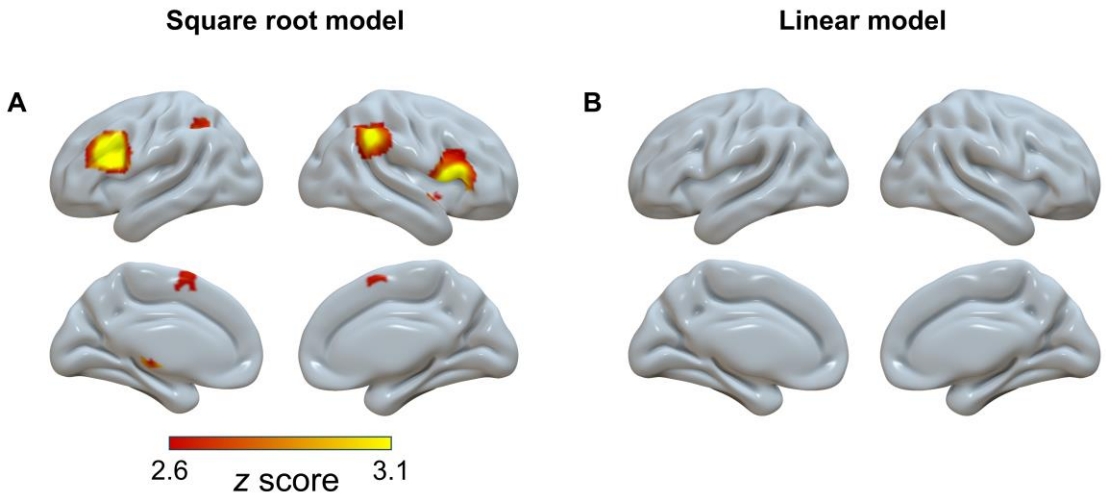

Fig. 5. Significant clusters (voxel-wise FWE-corrected, $p < 0.001$, voxels ≥ 10) showing square root pattern (A) and linear pattern (B) with age in the model fitting.

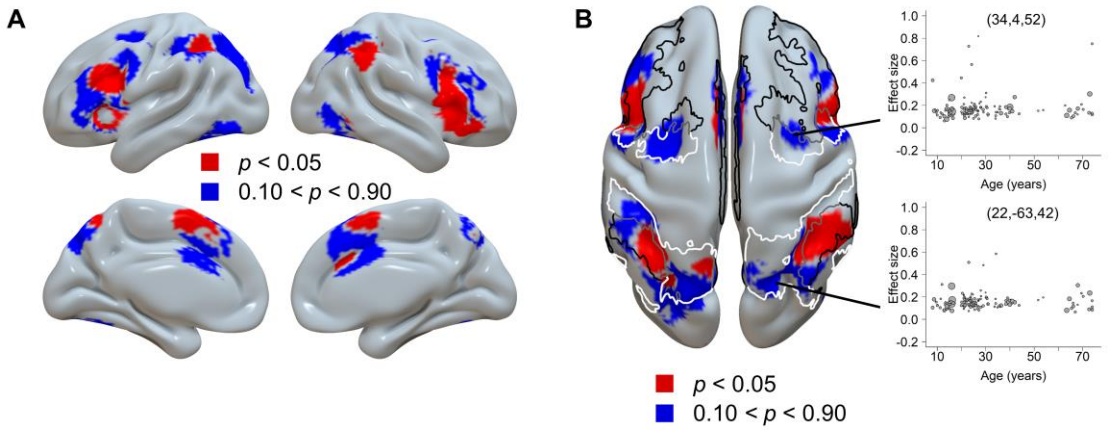

844

845 **Fig. 6**. Dissociated brain regions based on their trajectory patterns. A) The regions
846 following inverted U-shaped trajectories (red color) and non-U-shaped trajectories
847 (blue color). B) The axial view of the same results. The border lines display the fron-
848 toparietal control network (black), dorsal attention network (white), and their bound-
849 ary (gray) from Yeo's 7-network atlas[49]. Cingulo-opercular network was not plotted
850 due to its less clear dissociation among the two maps. The two scatter plots show two
851 example regions showing the non-U-shaped trajectory, one ([34, 4, 52]) representing a
852 peak region from the average brain activity analysis (Supplementary Table S3), and
853 the other ([22, −63, 42]) representing a region displaying a weak age-related change
854 from the contrast analysis with p between 0.49 and 0.51. The GAM analysis showed
855 that neither coordinate could be adequately fitted by a smoothed curve, with *p*s >
856 0.22.

857

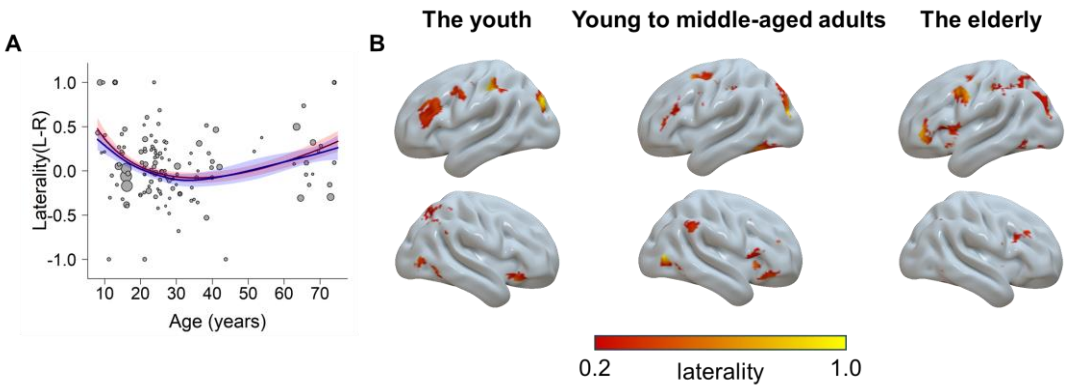

858

859 **Fig. 7**. The laterality as a function of age. A) The trajectory fitted with a square root

860 model (red) and the GAM (blue). Higher values mean more left-lateralized and lower

861 values mean more right-lateralized. B) Visualization of the laterality for each group.

862 Regions in the left hemisphere show the left laterality, and vice versa.

863

References

1. Cohen JD. Cognitive control: Core constructs and current considerations. In: *The Wiley handbook of cognitive control* (ed Egner T) (2017).
2. Miller EK, Cohen JD. An integrative theory of prefrontal cortex function. *Annu Rev Neurosci* **24**, 167-202 (2001).
3. Li Z, Goschl F, Yang G. Dissociated Neural Mechanisms of Target and Distractor Processing Facilitated by Expectations. *J Neurosci* **40**, 1997-1999 (2020).
4. Constantinidis C, Luna B. Neural Substrates of Inhibitory Control Maturation in Adolescence. *Trends Neurosci* **42**, 604-616 (2019).
5. Craik FI, Bialystok E. Cognition through the lifespan: mechanisms of change. *Trends Cogn Sci* **10**, 131-138 (2006).
6. Gupta R, Kar BR. Development of attentional processes in ADHD and normal children. *Prog Brain Res* **176**, 259-276 (2009).
7. Casey BJ, Getz S, Galvan A. The adolescent brain. *Dev Rev* **28**, 62-77 (2008).
8. Diamond A. Executive functions. *Annu Rev Psychol* **64**, 135-168 (2013).
9. Zanto TP, Gazzaley A. Attention and ageing. In: *The Oxford handbook of attention.*). Oxford University Press (2014).
10. Reuter-Lorenz PA, Cappell KA. Neurocognitive Aging and the Compensation Hypothesis. *Current Directions in Psychological Science* **17**, 177-182 (2008).
11. Association AP. Diagnostic and statistical manual of mental disorders : DSM-5.). 5th edn. American Psychiatric Association (2013).
12. Adnan A, Chen AJW, Novakovic-Agopian T, D'Esposito M, Turner GR. Brain Changes Following Executive Control Training in Older Adults. *Neurorehabil Neural Repair* **31**, 910-922 (2017).
13. Casey BJ, Tottenham N, Liston C, Durston S. Imaging the developing brain: what have we learned about cognitive development? *Trends Cogn Sci* **9**, 104-110 (2005).
14. Grady C. The cognitive neuroscience of ageing. *Nat Rev Neurosci* **13**, 491-505 (2012).
15. Weintraub S, *et al*. Cognition assessment using the NIH Toolbox. *Neurology* **80**, S54-64 (2013).
16. Ferguson HJ, Brunsdon VEA, Bradford EEF. The developmental trajectories of executive function from adolescence to old age. *Sci Rep* **11**, 1382 (2021).
17. Li SC, Hammerer D, Muller V, Hommel B, Lindenberger U. Lifespan development of stimulus-response conflict cost: similarities and differences between maturation and senescence. *Psychol Res* **73**, 777-785 (2009).

18. Erb CD, Germine L, Hartshorne JK. Cognitive control across the lifespan: Congruency effects reveal divergent developmental trajectories. *J Exp Psychol Gen* **152**, 3285-3291 (2023).
19. Brouwer RM, *et al.* Genetic variants associated with longitudinal changes in brain structure across the lifespan. *Nat Neurosci* **25**, 421-432 (2022).
20. Bethlehem RAI, *et al.* Brain charts for the human lifespan. *Nature*, (2022).
21. Li Q, Yang G, Li Z, Qi Y, Cole MW, Liu X. Conflict detection and resolution rely on a combination of common and distinct cognitive control networks. *Neurosci Biobehav Rev* **83**, 123-131 (2017).
22. Giedd JN, *et al.* Brain development during childhood and adolescence: a longitudinal MRI study. *Nat Neurosci* **2**, 861-863 (1999).
23. Crone EA, Dahl RE. Understanding adolescence as a period of social-affective engagement and goal flexibility. *Nat Rev Neurosci* **13**, 636-650 (2012).
24. Andrews-Hanna JR, Mackiewicz Seghete KL, Claus ED, Burgess GC, Ruzic L, Banich MT. Cognitive control in adolescence: neural underpinnings and relation to self-report behaviors. *PLoS One* **6**, e21598 (2011).
25. Veroude K, Jolles J, Croiset G, Krabbendam L. Changes in neural mechanisms of cognitive control during the transition from late adolescence to young adulthood. *Dev Cogn Neurosci* **5**, 63-70 (2013).
26. Wilk HA, Morton JB. Developmental changes in patterns of brain activity associated with moment-to-moment adjustments in control. *Neuroimage* **63**, 475-484 (2012).
27. Konrad K, *et al.* Development of attentional networks: an fMRI study with children and adults. *Neuroimage* **28**, 429-439 (2005).
28. Marsh R, *et al.* A developmental fMRI study of self-regulatory control. *Hum Brain Mapp* **27**, 848-863 (2006).
29. Bunge SA, Dudukovic NM, Thomason ME, Vaidya CJ, Gabrieli JD. Immature frontal lobe contributions to cognitive control in children: evidence from fMRI. *Neuron* **33**, 301-311 (2002).
30. Milham MP, *et al.* Attentional control in the aging brain: insights from an fMRI study of the stroop task. *Brain Cogn* **49**, 277-296 (2002).
31. Yaple ZA, Stevens WD, Arsalidou M. Meta-analyses of the n-back working memory task: fMRI evidence of age-related changes in prefrontal cortex involvement across the adult lifespan. *Neuroimage* **196**, 16-31 (2019).
32. Prakash RS, Erickson KI, Colcombe SJ, Kim JS, Voss MW, Kramer AF. Age-related differences in the involvement of the prefrontal cortex in attentional control. *Brain Cogn* **71**, 328-335 (2009).
33. Fernandez NB, Hars M, Trombetti A, Vuilleumier P. Age-related changes in attention control and their relationship with gait performance in older adults with high risk of falls. *Neuroimage* **189**, 551-559 (2019).

34. Sebastian A, *et al.* Differential effects of age on subcomponents of response inhibition. *Neurobiology of aging* **34**, 2183-2193 (2013).
35. Verhaeghen P, Cerella J. Aging, executive control, and attention: a review of meta-analyses. *Neurosci Biobehav Rev* **26**, 849-857 (2002).
36. Verhaeghen P. *The elements of cognitive aging: Meta-analyses of age-related differences in processing speed and their consequences*. OUP USA (2014).
37. Wood G, Ischebeck A, Koppelstaetter F, Gotwald T, Kaufmann L. Developmental trajectories of magnitude processing and interference control: an FMRI study. *Cereb Cortex* **19**, 2755-2765 (2009).
38. Hart H, Radua J, Nakao T, Mataix-Cols D, Rubia K. Meta-analysis of functional magnetic resonance imaging studies of inhibition and attention in attention-deficit/hyperactivity disorder: exploring task-specific, stimulant medication, and age effects. *JAMA psychiatry* **70**, 185-198 (2013).
39. Zhang Z, Peng P, Eickhoff SB, Lin X, Zhang D, Wang Y. Neural substrates of the executive function construct, age-related changes, and task materials in adolescents and adults: ALE meta-analyses of 408 fMRI studies. *Dev Sci* **24**, e13111 (2021).
40. Long J, Song X, Wang Y, Wang C, Huang R, Zhang R. Distinct neural activation patterns of age in subcomponents of inhibitory control: A fMRI meta-analysis. *Front Aging Neurosci* **14**, 938789 (2022).
41. Yarkoni T, Poldrack RA, Nichols TE, Van Essen DC, Wager TD. Large-scale automated synthesis of human functional neuroimaging data. *Nat Methods* **8**, 665-670 (2011).
42. Nee DE, Wager TD, Jonides J. Interference resolution: insights from a meta-analysis of neuroimaging tasks. *Cogn Affect Behav Neurosci* **7**, 1-17 (2007).
43. Botvinick MM, Cohen JD, Carter CS. Conflict monitoring and anterior cingulate cortex: an update. *Trends Cogn Sci* **8**, 539-546 (2004).
44. Kerns JG, Cohen JD, MacDonald AW, 3rd, Cho RY, Stenger VA, Carter CS. Anterior cingulate conflict monitoring and adjustments in control. *Science* **303**, 1023-1026 (2004).
45. Simonsohn U. Two Lines: A Valid Alternative to the Invalid Testing of U-Shaped Relationships With Quadratic Regressions. *Advances in Methods and Practices in Psychological Science* **1**, 538-555 (2018).
46. Zuo XN, *et al.* Growing together and growing apart: regional and sex differences in the lifespan developmental trajectories of functional homotopy. *J Neurosci* **30**, 15034-15043 (2010).
47. Coupe P, Catheline G, Lanuza E, Manjon JV, Alzheimer's Disease Neuroimaging I. Towards a unified analysis of brain maturation and aging across the entire lifespan: A MRI analysis. *Hum Brain Mapp* **38**, 5501-5518 (2017).

48. Amlien IK, Sneve MH, Vidal-Pineiro D, Walhovd KB, Fjell AM. The Lifespan Trajectory of the Encoding-Retrieval Flip: A Multimodal Examination of Medial Parietal Cortex Contributions to Episodic Memory. *J Neurosci* **38**, 8666-8679 (2018).
49. Yeo BT, *et al.* The organization of the human cerebral cortex estimated by intrinsic functional connectivity. *J Neurophysiol* **106**, 1125-1165 (2011).
50. De Luca CR, Leventer RJ. Developmental trajectories of executive functions across the lifespan. In: *Executive functions and the frontal lobes*). Psychology Press (2010).
51. Vaidya CJ, Bunge SA, Dudukovic NM, Zalecki CA, Elliott GR, Gabrieli JD. Altered neural substrates of cognitive control in childhood ADHD: evidence from functional magnetic resonance imaging. *The American journal of psychiatry* **162**, 1605-1613 (2005).
52. Robertson BD, Hiebert NM, Seergobin KN, Owen AM, MacDonald PA. Dorsal striatum mediates cognitive control, not cognitive effort per se, in decision-making: An event-related fMRI study. *Neuroimage* **114**, 170-184 (2015).
53. Hsu CL, *et al.* Aerobic exercise promotes executive functions and impacts functional neural activity among older adults with vascular cognitive impairment. *Br J Sports Med* **52**, 184-191 (2018).
54. , (!!! INVALID CITATION !!!).
55. Brenhouse HC, Andersen SL. Developmental trajectories during adolescence in males and females: a cross-species understanding of underlying brain changes. *Neurosci Biobehav Rev* **35**, 1687-1703 (2011).
56. Gogtay N, *et al.* Dynamic mapping of human cortical development during childhood through early adulthood. *Proc Natl Acad Sci U S A* **101**, 8174-8179 (2004).
57. Luna B, Marek S, Larsen B, Tervo-Clemmens B, Chahal R. An integrative model of the maturation of cognitive control. *Annu Rev Neurosci* **38**, 151-170 (2015).
58. Shaw P, *et al.* Neurodevelopmental trajectories of the human cerebral cortex. *J Neurosci* **28**, 3586-3594 (2008).
59. Grimm KJ, Ram N, Estabrook R. *Growth Modeling: Structural Equation and Multilevel Modeling Approaches*. Guilford Publications (2016).
60. Verissimo J, Verhaeghen P, Goldman N, Weinstein M, Ullman MT. Evidence that ageing yields improvements as well as declines across attention and executive functions. *Nat Hum Behav* **6**, 97-110 (2022).
61. D'Mello AM, Gabrieli JDE, Nee DE. Evidence for Hierarchical Cognitive Control in the Human Cerebellum. *Curr Biol* **30**, 1881-1892 e1883 (2020).
62. Shine JM, Lewis LD, Garrett DD, Hwang K. The impact of the human thalamus on brain-wide information processing. *Nat Rev Neurosci* **24**, 416-430 (2023).

63. Cole MW, Reynolds JR, Power JD, Repovs G, Anticevic A, Braver TS. Multi-task connectivity reveals flexible hubs for adaptive task control. *Nat Neurosci* **16**, 1348-1355 (2013).
64. Zhou Y, Friston KJ, Zeidman P, Chen J, Li S, Razi A. The Hierarchical Organization of the Default, Dorsal Attention and Salience Networks in Adolescents and Young Adults. *Cereb Cortex* **28**, 726-737 (2018).
65. Petersen SE, Posner MI. The attention system of the human brain: 20 years after. *Annu Rev Neurosci* **35**, 73-89 (2012).
66. Badre D, Nee DE. Frontal Cortex and the Hierarchical Control of Behavior. *Trends Cogn Sci* **22**, 170-188 (2018).
67. Dixon ML, *et al.* Heterogeneity within the frontoparietal control network and its relationship to the default and dorsal attention networks. *Proc Natl Acad Sci U S A* **115**, E1598-E1607 (2018).
68. Sydnor VJ, *et al.* Intrinsic activity development unfolds along a sensorimotor-association cortical axis in youth. *Nat Neurosci* **26**, 638-649 (2023).
69. Raz N, *et al.* Selective aging of the human cerebral cortex observed in vivo: differential vulnerability of the prefrontal gray matter. *Cereb Cortex* **7**, 268-282 (1997).
70. Fjell AM, Walhovd KB. Structural brain changes in aging: courses, causes and cognitive consequences. *Rev Neurosci* **21**, 187-221 (2010).
71. Kaplan L, Chow BW, Gu C. Neuronal regulation of the blood-brain barrier and neurovascular coupling. *Nat Rev Neurosci* **21**, 416-432 (2020).
72. Lipecz A, *et al.* Age-related impairment of neurovascular coupling responses: a dynamic vessel analysis (DVA)-based approach to measure decreased flicker light stimulus-induced retinal arteriolar dilation in healthy older adults. *Geroscience* **41**, 341-349 (2019).
73. Zlokovic BV. Neurovascular pathways to neurodegeneration in Alzheimer's disease and other disorders. *Nat Rev Neurosci* **12**, 723-738 (2011).
74. Montala-Flaquer M, Canete-Masse C, Vaque-Alcazar L, Bartres-Faz D, Pero-Cebollero M, Guardia-Olmos J. Spontaneous brain activity in healthy aging: An overview through fluctuations and regional homogeneity. *Front Aging Neurosci* **14**, 1002811 (2022).
75. Cappell KA, Gmeindl L, Reuter-Lorenz PA. Age differences in prefontal recruitment during verbal working memory maintenance depend on memory load. *Cortex* **46**, 462-473 (2010).
76. Zanto TP, Gazzaley A. Cognitive Control and the Ageing Brain. In: *The Wiley Handbook of Cognitive Control* (ed Egner T) (2017).
77. Park DC, Reuter-Lorenz P. The adaptive brain: aging and neurocognitive scaffolding. *Annu Rev Psychol* **60**, 173-196 (2009).

78. Hoffman P, Morcom AM. Age-related changes in the neural networks supporting semantic cognition: A meta-analysis of 47 functional neuroimaging studies. *Neurosci Biobehav Rev* **84**, 134-150 (2018).
79. Langenecker SA, Nielson KA, Rao SM. fMRI of healthy older adults during Stroop interference. *NeuroImage* **21**, 192-200 (2004).
80. Cabeza R. Hemispheric asymmetry reduction in older adults: the HAROLD model. *Psychol Aging* **17**, 85-100 (2002).
81. Dolcos F, Rice HJ, Cabeza R. Hemispheric asymmetry and aging: right hemisphere decline or asymmetry reduction. *Neurosci Biobehav Rev* **26**, 819-825 (2002).
82. Zhang HY, Chen WX, Jiao Y, Xu Y, Zhang XR, Wu JT. Selective vulnerability related to aging in large-scale resting brain networks. *PLoS One* **9**, e108807 (2014).
83. Thatcher RW, Walker RA, Giudice S. Human cerebral hemispheres develop at different rates and ages. *Science* **236**, 1110-1113 (1987).
84. Cabeza R, *et al.* Age-related differences in neural activity during memory encoding and retrieval: a positron emission tomography study. *J Neurosci* **17**, 391-400 (1997).
85. Grady CL, Bernstein LJ, Beig S, Siegenthaler AL. The effects of encoding task on age-related differences in the functional neuroanatomy of face memory. *Psychol Aging* **17**, 7-23 (2002).
86. Albajes-Eizagirre A, Solanes A, Vieta E, Radua J. Voxel-based meta-analysis via permutation of subject images (PSI): Theory and implementation for SDM. *Neuroimage* **186**, 174-184 (2019).
87. Sowell ER, Thompson PM, Toga AW. Mapping changes in the human cortex throughout the span of life. *Neuroscientist* **10**, 372-392 (2004).
88. Thompson SG, Higgins JP. How should meta-regression analyses be undertaken and interpreted? *Stat Med* **21**, 1559-1573 (2002).
89. Cumpston M, *et al.* Updated guidance for trusted systematic reviews: a new edition of the Cochrane Handbook for Systematic Reviews of Interventions. *Cochrane Database Syst Rev* **10**, ED000142 (2019).
90. Lu J, Yao J, Zhou Z, Wang XT. Age effects on delay discounting across the lifespan: A meta-analytical approach to theory comparison and model development. *Psychological Bulletin* **149**, 447-486 (2023).
91. Page MJ, *et al.* The PRISMA 2020 statement: an updated guideline for reporting systematic reviews. **88**, 105906 (2021).
92. Lancaster JL, *et al.* Bias between MNI and talairach coordinates analyzed using the ICBM-152 brain template. *Human Brain Mapping* **28**, 1194-1205 (2007).
93. Turkeltaub PE, Eickhoff SB, Laird AR, Fox M, Wiener M, Fox P. Minimizing within-experiment and within-group effects in activation likelihood estimation meta-analyses. *Human Brain Mapping* **33**, 1-13 (2012).

94. Eickhoff SB, Bzdok D, Laird AR, Kurth F, Fox PT. Activation likelihood estimation meta-analysis revisited. *NeuroImage* **59**, 2349-2361 (2012).
95. Radua J, Mataix-Cols D. Meta-analytic methods for neuroimaging data explained. *Biol Mood Anxiety Disord* **2**, 6 (2012).
96. Hedges LV. Distribution theory for Glass's estimator of effect size and related estimators. *Journal of Educational Statistics* **6**, 107-128 (1981).
97. Radua J, *et al.* A new meta-analytic method for neuroimaging studies that combines reported peak coordinates and statistical parametric maps. *Eur Psychiat* **27**, 605-611 (2012).
98. Egger M, Smith GD, Phillips AN. Meta-analysis: principles and procedures. *BMJ (Clinical research ed)* **315**, 1533-1537 (1997).
99. Higgins JP, Thompson SG, Deeks JJ, Altman DG. Measuring inconsistency in meta-analyses. *BMJ (Clinical research ed)* **327**, 557-560 (2003).
100. Wood SN. mgcv: GAMs and generalized ridge regression for R. *J R news* **1**, 20-25 (2001).
101. Zuo XN, He Y, Betzel RF, Colcombe S, Sporns O, Milham MP. Human Connectomics across the Life Span. *Trends Cogn Sci* **21**, 32-45 (2017).
102. Bethlehem RAI, *et al.* Brain charts for the human lifespan. *Nature* **604**, 525-533 (2022).
103. Ochieng' Odhiambo F. Comparative Study of Various Methods of Handling Missing Data. *Mathematical Modelling and Applications* **5**, (2020).
104. Sandhu AT, Kohsaka S, Turakhia MP, Lewis EF, Heidenreich PA. Evaluation of Quality of Care for US Veterans With Recent-Onset Heart Failure With Reduced Ejection Fraction. *JAMA Cardiol* **7**, 130-139 (2022).
105. Seghier ML. Laterality index in functional MRI: methodological issues. *Magn Reson Imaging* **26**, 594-601 (2008).
106. Yang G. guochun-yang/Cognitive_Control_Developmental_Trajectory: Release_20240711 (Lifespan).). Zenodo (2024).